Journal of Proteomics 280 (2023) 104896

Contents lists available at ScienceDirect

Journal of Proteomics

journal homepage: www.elsevier.com/locate/jprot

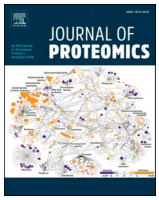

Proteomic and N-glycoproteomic analyses of total subchondral bone protein in patients with primary knee osteoarthritis

Gangning Feng [a,b,1], Yong Zhou [e,1], Jiangbo Yan [a,b], Zheng Wang [c], Yong Yang [b], Weidong Zhao [b], Na Wang [d], Zhidong Lu [b], Yaogeng Chen [f], Qunhua Jin [b,g,*]

[a] Clinical College, Ningxia Medical University, Yinchuan, PR China
[b] Orthopedics Ward 3, The General Hospital of Ningxia Medical University, 804 Shengli South Street, Yinchuan 750004, Ningxia, PR China
[c] Orthopedics Department Trauma Ward 2, The General Hospital of Ningxia Medical University, 804 Shengli South Street, Yinchuan 750004, Ningxia, PR China
[d] Department of Hand Foot Ankle Surgical Ward, The General Hospital of Ningxia Medical University, 804 Shengli South Street, Yinchuan 750004, Ningxia, PR China
[e] Department of Hand Surgical Ward, DaXing Hospital of Xi'an, 353 LaoDong North Street, Xian 710082, Shaanxi, PR China
[f] Department of Ningxia Medical University, Yinchuan 750004, Ningxia, PR China
[g] Institute of Medical Sciences, General Hospital of Ningxia Medical University, Yinchuan 750004, Ningxia, PR China

ARTICLE INFO

Keywords:
Primary knee osteoarthritis
Proteomics
N-glycoproteomics
Subchondral bone

ABSTRACT

N-glycosylation is an important post-translational modification necessary to maintain the structural and functional properties of proteins. Impaired N-glycosylation has been observed in several diseases. It is significantly modified by the state of cells and is used as a diagnostic or prognostic indicator for multiple human diseases, including cancer and osteoarthritis (OA). Aim of the study was to explore the N-glycosylation levels of subchondral bone proteins in patients with primary knee OA (KOA) and screen for potential biological markers for the diagnosis and treatment of primary KOA. A comparative analysis of total protein N-glycosylation under the cartilage was performed in medial subchondral bone (MSB, $N = 5$) and lateral subchondral bone (LSB, $N = 5$) specimens from female patients with primary KOA. To analyse the N-glycosylation sites of the proteins, non-labelled quantitative proteomic and N-glycoproteomic analyses were performed based on liquid chromatography-tandem mass spectrometry (LC-MS/MS) data. Parallel reaction monitoring (PRM) validation experiments were carried out on differential N-glycosylation sites of proteins in selected specimens, including MSB ($N = 5$) and LSB ($N = 5$), from patients with primary KOA. In total, 1149 proteins with 1369 unique N-chain glycopeptides were detected, and 1215 N-glycosylation sites were found, in which ptmRS scores for 1163 N-glycosylation sites were ≥ 0.9. In addition, N-glycosylation of the total protein in MSB compared to that in LSB was identified, in which 295 N-glycosylation sites were significantly different, including 75 upregulated and 220 downregulated N-glycosylation sites in MSB samples. Importantly, Gene Ontology (GO) and Kyoto Encyclopaedia of Genes and Genomes (KEGG) pathway enrichment analyses of proteins with differential N-glycosylation sites showed that they were primarily associated with metabolic pathways including ECM-receptor interactions, focal adhesion, protein digestion and absorption, amoebiasis, and complement and coagulation cascades. Finally, PRM experiments confirmed the N-glycosylation sites of collagen type VI, alpha 3 (COL6A3, VAVVQHAPSESVDN[+3]ASMPPVK), aggrecan core protein (ACAN, FTFQEAAN[+3]EC[+57]R, TVYVHAN[+3]QTGYPDPSSR), laminin subunit gamma-1 (LAMC1, IPAIN[+3]QTITEANEK), matrix-remodelling-associated protein 5 (MXRA5, ITLHEN[+3]R), cDNA, FLJ92775, highly similar to *Homo sapiens* melanoma cell adhesion molecule (MCAM), mRNA (B2R642, C[+57]VASVPSIPGLN[+3]R), and aminopeptidase fragment (Q59E93, AEFN[+3]ITLIHPK) in the array data of the top 20 N-glycosylation sites. These abnormal N-glycosylation patterns provide reliable insights for the development of diagnostic and therapeutic methods for primary KOA.

* Corresponding author at: Orthopedics Ward 3, The General Hospital of Ningxia Medical University, 804 Shengli South Street, Yinchuan 750004, Ningxia, PR China.
E-mail address: jinqunhua2020@163.com (Q. Jin).
[1] These authors contributed equally to this work.

https://doi.org/10.1016/j.jprot.2023.104896
Received 21 November 2022; Received in revised form 25 March 2023; Accepted 26 March 2023
Available online 5 April 2023

1. Introduction

Osteoarthritis (OA) is a major disease affecting the musculoskeletal system that induces tissue damage to the whole joint and constitutes a main factor causing disability in the elderly. Between 1990 and 2017, the incidence of OA has increased by 102%, with the aging population being the primary concern. The global age-standardised incidence rate (ASIR) of OA is increasing at an annual rate of 0.32% [1]. In China, the prevalence of OA is 14.6% [2], with 13.7% in southwest China and 10.8% in northwest China [3].

Among the joint structures involved in OA, subchondral bone and cartilage are the most important functional complexes of bone-cartilage units, participating in the pathological process of OA at the molecular and mechanical levels [4]. Subchondral bone is the main structure that regulates the pathogenic mechanisms of OA [5]. In early OA, abnormal mechanical stress and other factors induce microdamage to the subchondral bone and increase subchondral bone remodelling, and osteoclasts promote bone resorption, subchondral bone plate thinning, and trabecular separation. In the advanced stages of OA, bone remodelling is weakened, osteoblast-mediated bone formation is strengthened, subchondral plate and bone trabecular thickening occurs, and angiogenesis increases, manifesting as subchondral osteosclerosis, which affects the degeneration of the overlying cartilage [6]. Subchondral sclerosis is the most direct manifestation of bone conversion in OA. However, the exact mechanism by which abnormal subchondral bone formation causes osteosclerosis remains unknown. It is generally accepted that the subchondral bone structure adapts to abnormal mechanical stresses through bone remodelling. Localised osteosclerosis and non-sclerosing regions can result in an imbalanced distribution of shear stress, creating heterogeneity in the subchondral bone-cartilage complex, tearing the attached cartilage, and triggering fibrosis. The meniscal instability model of OA established by the *Sost* gene (encoding the sclerostin protein) in mice demonstrated that increased bone density and hardness under the cartilage are prerequisites for OA progression [7]. In addition, compared to the non-weight-bearing area, the subchondral bone-bone interface shows significant chondrocyte hypertrophy and endochondral ossification, induced remodelling, enhanced subchondral osteosclerosis, and more severe cartilage degeneration in the weight-bearing area [8]. Although numerous biomechanical and biochemical studies have focused on elucidating the mechanism by which OA occurs and develops, its pathogenesis remains unclear.

Glycosylation is the study of the biological functions of glycan chains in interactions with proteins and lipid molecules; typical glycosylation changes are o-chain and n-chain glycosylation, which are applied to molecular-based research in the biomedical field [9–11]. There are two types of glycans attached to glycoproteins: N-glycans (linked to asparagine residues by nitrogen atoms) and O-glycans (linked to serine or threonine residues) [12]. N-glycosylation in proteins is highly diverse, with high stability in a specific pathophysiological state in a given individual and high levels of variation that may result from pathological conditions and aging [13,14]. With the development of mass spectrometry (MS), glycoproteomics has been widely used to provide critical insights into the underlying molecular basis of biological systems, disease diagnosis, and prognosis [15–17]. Currently, N-glycosylation is considered an efficient and feasible indicator of early diagnosis and prognosis of multiple diseases. It has important significance in the early diagnosis and survival evaluation [18]. In addition to cancer, the altered expression of N-glycosylation in autoimmune diseases, including rheumatoid arthritis [19] and inflammatory bowel disease (IBD) [20], has been extensively studied.

OA is commonly diagnosed as an aging-related and degenerative disease [21]. Current reports indicate that OA is associated with mechanical damage [22], and is also correlated with active and dynamic changes in the joint tissue caused by an imbalance between repair and destruction [23]. The occurrence and development of OA are closely associated with the aging of cells [24]. N-glycosylation contributes to multiple molecular mechanisms of cellular senescence [25]. In addition, N-glycosylation contributes to the regulatory mechanism between osteoprotegerin (OPG) and osteoclasts in the subchondral bone in OA cases [26]. OPG is an N-glycosylated protein comprising 401 amino acids [27,28] with high expression levels in several tissues [27]. Previous studies have also indicated N-glycan alterations in the cartilage of a rabbit model of surgically induced OA [29]. Recent data assessing the N-glycosylation biomarkers of canine OA demonstrated that they can be used as diagnostic markers of canine OA [30].

Ahlback et al. [31] showed that in 85% of cases, joint degeneration (wear and tear) involved only one compartment. Hernborg et al. [32] concluded that degeneration begins in the medial compartment in 90% of the cases. This may be related to the evolutionary history of humans, in which only the human knee joint can be fully straightened, whereas the medial condyle of the tibial platform may form a stress concentration point.

In the present study, comprehensive non-labelled quantitative proteomic and N-glycoproteomic analyses of medial subchondral bone (MSB, $N = 5$) and lateral subchondral bone (LSB; $N = 5$) samples were performed in patients with primary knee OA (KOA). Liquid chromatography-tandem mass spectrometry (LC-MS/MS) was used to study the protein and N-glycosylation expression levels. Next, parallel reaction monitoring (PRM) validation experiments were performed on different sites of the selected specimens, including MSB ($N = 5$) and LSB ($N = 5$). To the best of our knowledge, this is the first study to examine total subchondral bone protein N-glycosylation in patients with primary KOA and screen potential biological markers for the diagnosis and treatment of primary KOA.

2. Materials and methods

2.1. Clinical samples

Ten female patients with primary KOA who underwent total knee replacement between October 2020 and March 2021 at the General Hospital of Ningxia Medical University (Yinchuan, China) were included. Patients with secondary arthritis resulting from rheumatoid arthritis, trauma, and/or serious liver or kidney disease were excluded. The mean age of patients was 68.4 (range, 64–72) years. Body mass index (BMI) was determined and OA severity was rated based on the Kelgren-Lawrence Radiological Grading Criteria. The characteristics of all patients are shown in Fig. 1 and Table 1. During surgery, five patients were randomly selected to provide LSB samples and the other five patients were selected for MSB. Informed consent was obtained from all enrolled patients. This study was approved by the Ethics Committee of the General Hospital of Ningxia Medical University (approval no. KYLL-2021-575).

2.2. Protein analysis

Ten tissue samples (two groups with five samples in each group) were homogenised in liquid nitrogen. Approximately 20 mg of the homogenate was lysed with 200 μL of lysis buffer (4% sodium dodecylsulphate [SDS] and 100 mM dithiothreitol [DTT] in 150 mM Tris-HCl, pH 8.0). This was followed by boiling, ultrasonication, and centrifugation (16,000 ×*g* for 15 min). The protein content of the supernatant was assessed using a bicinchoninic acid (BCA) Protein Assay kit (Bio-Rad, Hercules, CA, USA). The proteins were digested as described by Wisniewski et al. [33] and others [34,35]. Then, 100 μL of 0.05 M iodoacetamide was added to block the reduced cysteine residues and the samples were incubated in the dark for 20 min. The filter was then washed thrice with 100 μL UA buffer (8 M urea, 150 mM Tris-HCl, pH 8.0), followed by washing twice with 100 μL of 50 mM NH4HCO3. Finally, the protein suspension was digested overnight at 37 °C in 40 μL of 50 mM NH4HCO3 (Promega) (protein:trypsin, 40:1) and then centrifuged at 12,000 ×*g* for 10 min to collect peptides. The vacuum-

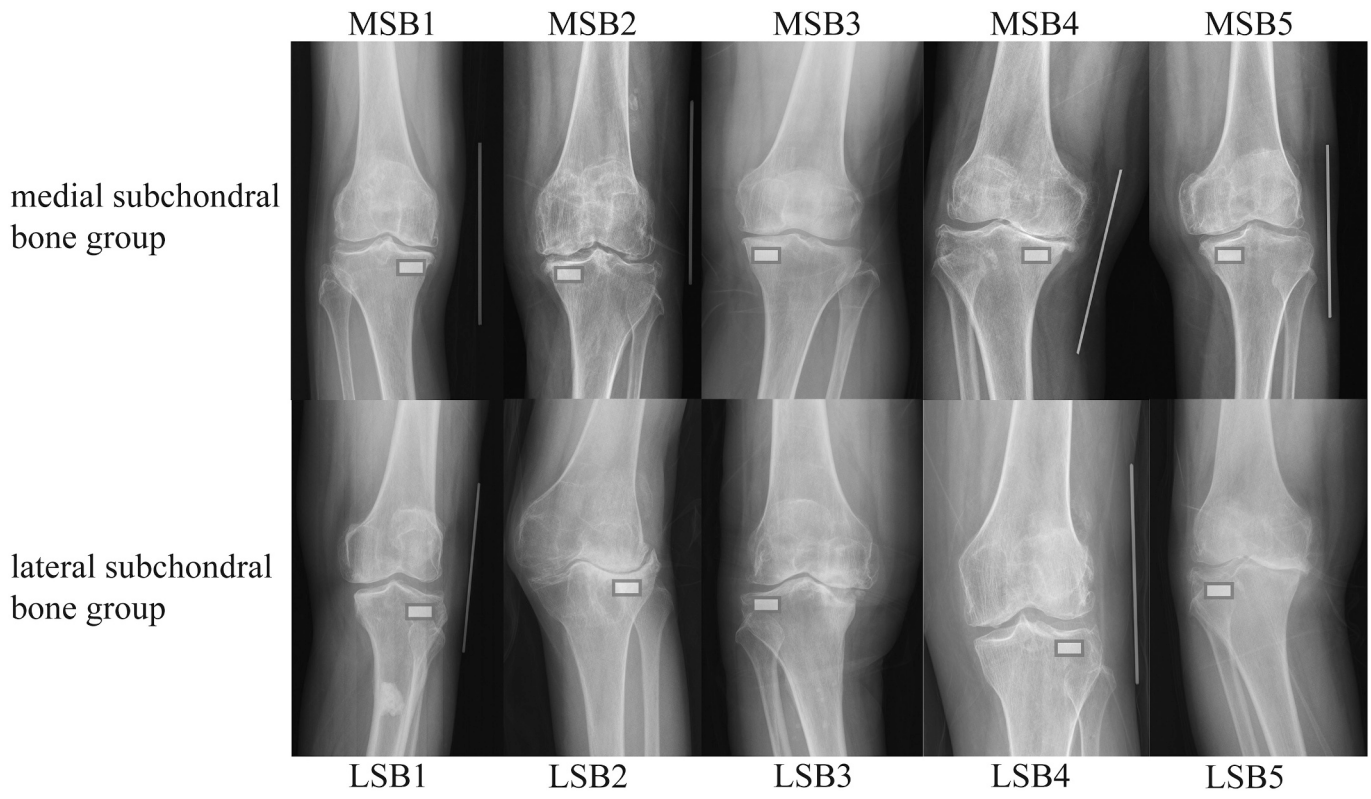

Fig. 1. Clinical Imaging data of subjects. Imaging information of patients with primary KOA in the MSB (N = 5) and LSB groups (N = 5).

Table 1
Clinical information of the subjects.

	MSB group	LSB group	*p* value
n	5	5	
Age (years)	68 ± 2.8	69.4 ± 4.0	0.543
Gender (F/M)	5/0	5/0	
Weight (Kg)	64.4 ± 9.1	60.2 ± 6.1	0.418
Height (cm)	156.6 ± 3,2	156.8 ± 4.1	0.934
BMI (kg/m^2)	26.2 ± 2.6	24.4 ± 1.6	0.245
K-L grade	4(5)	4(5)	

dried peptide concentration was the determined using a Nanodrop device (Thermo Fisher Scientific) at OD280. The resulting peptides underwent acidification with 10% trifluoroacetic acid (TFA) and desalting with a C18 cartridge (Thermo Scientific).

2.3. Glycopeptide enrichment and deglycosylation

Tryptic peptides (400 μg) were transferred to a YM-30 filtration unit and treated for 1 h with a lectin mixture made of 90 μg ConA, 90 μg WGA, and 90 μg RCA120 in 36 μL of 2× binding buffer [33,36]. Then, the specimens were centrifuged (14,000 ×g for 10 min), and lectin-bound peptides were washed four times with 200 μL binding buffer and washed twice with 50 μL of 40 mM NH4HCO3 in [18]^{18}O water (Sigma). Deglycosylation was performed by adding 2 μL of PNGase F (1 U/μL in ^{18}O water) (Roche) in 40 μL of 40 mM NH4HCO3 in [18]O water, which was followed by a 3-h incubation at 37 °C. The deglycosylated peptides were centrifuged, and filters were washed twice with 50 μL of 40 mM NH4HCO3. After elution, the specimens were dried for LC-MS/MS.

2.4. LC-MS/MS

Chromatographic separation was performed using a nanolitre flow rate Easy nLC 1200 chromatographic system (Thermo Scientific) to obtain appropriate amounts of peptides per sample. Buffer: Solution A was 0.1% formic acid in water, and solution B was a mixed solution of 0.1% formic acid, acetonitrile, and water (95% acetonitrile). The column was equilibrated with a 100% liquid solution (A). The samples were injected into the trap Column (100 μm × 20 mm, 5 μm, C18, Dr. Maisch GmbH) and then subjected to a chromatographic column (75 μm × 150 mm, 3 μm, C18, Dr. Maisch GmbH) for gradient separation with a flow rate of 300 nL/min.

For liquid phase separation, the gradients were as follows:

Time (min)	B-liquid linear gradient (%)
0–2	2–5%
2–75	5–28%
75–80	28–40%
82	40–100%
82–90	100%

MS analysis of the peptides was performed using a Q-Exactive HF-X (Thermo Scientific) for a90-min analysis. The detection mode was positive ion, the precursor scanning range was 350–1800 m/z, the primary mass spectral resolution was 60,000 @m/z 200, and the Level 1 Maximum IT was 50 ms. The secondary mass spectrum (MS2) of each peptide precursor ion is acquired by means of a MS2 scan.

2.5. Sequence database search and data analysis

MS data analysis was performed using MaxQuant v1.6.1.0. UniProt-*Homo sapiens* [9606]-203,800-202201Fasta was used to match the MS data. Two missed cleavage sites were allowed, with mass tolerance of 4.5 and 20 ppm for the precursor and fragment ions, respectively. Carbamidomethylation of cysteine residues is considered as a fixed

modification, whereas N-terminal acetylation, methionine oxidation, and asparagine deamidation ([18]O) are variable modifications. A false discovery rate (FDR) < 0.01 at the site, peptide-spectrum-matched, and protein levels were considered statistically significant.

2.6. Bioinformatic analysis

For glycoproteomic data, *t*-test (*P*-value) and fold change (FC) were determined. We also performed Qvality q-value and Percolator q-value tests; q < 0.01 was considered statistically significant, and hierarchical clustering was used to group the expression data. For sequence annotation, Kyoto Encyclopaedia of Genes and Genomes (KEGG) and Gene Ontology (GO) analyses were performed using Fisher's exact test and FDR correction for multiple testing. Pathways enriched in GO and KEGG were considered statistically significant at $p < 0.05$, and the STRING database was used to generate protein-protein interaction (PPI) networks using the R language and R packages.

2.7. PRM analysis

To verify the protein expression levels obtained using iTRAQ/TMT/label-free analysis, the expression levels of the selected proteins were further quantified using LC-PRM/MS. [37]

Briefly, peptides were prepared according to the iTRAQ/TMT/label-free protocol, and raw data were analysed using Skyline (MacCoss Lab, University of Washington) [38] to obtain the signal intensities of individual peptide sequences.

3. Results

3.1. Protein identification and quantification

MS was used to detect 1149 proteins and 3514 unique peptides, including 1369-N glycosylated peptides and 1215 N-glycosylation sites, and ptmRSscore [39,40] for 1163 N-glycosylation sites was ≥0.9. (Table 2, Supplementary Table 1). As for protein identification, experimental data were first screened to ensure that signals are detected in at least three patients in samples corresponding to the identification of N-glycosylation sites, and statistical analysis was then performed, where N-glycosylation sites with fold-change>2 (upregulation) and *P*-value<0.05 were considered as significant differentially expressed sites. The Qvality q-value and Percolator q-value tests were also performed, and q < 0.01 was considered statistically significant. Comparison of the N-glycosylation sites between medial and LSB samples showed that there were 75 upregulated and 220 downregulated N-glycosylation sites in the medial subchondral total protein. There were 295 N-glycosylation sites with significant differences between the two groups, as well as 58 with or without differences (Table 3, Supplementary Table 2). In the analysis with or without differences in the quantitative results, that is the intensity of five patients in samples from one of the two comparison groups was not detected, whereas the other group had at least four patients in the samples.

3.2. N-glycosylation site analysis

A comparative analysis was performed on all N-glycosylation sites (ptmRSscore≥0.9) identified between the groups. The array data of the two groups were analysed using PCA, as shown in Fig. 2A. The fold change in modified site expression between the two sets of specimens and *t*-test-derived *P*-values were used to generate a volcano plot to display between-group differences. The abscissa and axes represent fold changes and P-values, respectively. The volcano plot depicts the relative number of modification sites in the MSB and LSB groups, where the red and green dots indicate significant upregulation and downregulation of the modification sites, respectively (Fig. 2B). The results of the Venn plots for the two groups are shown in Fig. 3A. A cluster heatmap analysis of the differences in glycosylation sites between the two groups was performed (Fig. 3B). Specific data are presented in the appendix (Supplementary Table 2).

3.3. Bioinformatics analysis

As N-glycosylated proteins were detected in this study, and several proteins exhibited multiple N-glycosylation sites, variations in different N-glycosylation sites should be assessed. In addition, the upregulation and downregulation of differentially N-glycosylated proteins could be defined; thus, only proteins corresponding to different sites in each comparison group (without fold-change differences) were analysed. The results of GO enrichment analysis of proteins with significantly different sites are shown in Fig. 4A. Fig. 4C illustrates the GO annotation results at level 2, where each abscissa is the term of level 2, the left coordinate is the count (annotated to the number of differentially expressed proteins), and the right coordinate is the ratio (number of differentially expressed proteins annotated to the term/total number of differentially expressed proteins with GO annotation). Different colours represent the three major categories of GO: biological process (BP), molecular function (MF), and cellular components (CC). Each column is marked by a specific count. Next, the KEGG pathway enrichment analysis was performed to examine proteins with significantly different sites (Fig. 4B).

3.4. Protein-protein interaction (PPI) network analysis

A PPI network of proteins with significantly different sites was generated (Fig. 5). Details of the PPI network analysis are provided in the Appendix (Supplementary Table 5).

3.5. Bioinformatics analysis of the top 20 N-glycosylation sites of proteins with the most significant differences

Based on the results of the statistical analysis, the top 20 N-glycosylation sites of proteins with the largest differences were selected for bioinformatics analysis. The array data for the top 20 N-glycosylation sites of proteins are shown in Table 4 (Supplementary Table 3). A volcano plot of the top 20 N-glycosylation sites of proteins is shown in Fig. 6A, a heatmap of the top 20 N-glycosylation sites of proteins is shown in Fig. 6B, and the results of GO and KEGG enrichment analyses of the top 20 N-glycosylation sites of proteins are presented in Fig. 6C–E and Fig. 6F, respectively.

3.6. Motif analysis

The identification of conserved motifs of modified proteins for protein post-translational modification and modification site prediction, as well as the discovery of cell signalling pathways, has critical implications. Therefore, motif analysis of the filtered and reliable sites was performed (Fig. 7).

3.7. PRM validation of the results

PRM experiments confirmed the N-glycosylation sites of collagen type VI, alpha 3 (COL6A3, VAVVQHAPSESVDN[+3]ASMPPVK), aggrecan core protein (ACAN, FTFQEAAN[+3]EC[+57]R, TVYVHAN[+3]QTGYPDPSSR), laminin subunit gamma-1 (LAMC1, IPAIN[+3]QTITEANEK), matrix-remodelling-associated protein 5 (MXRA5, ITLHEN[+3]R), cDNA, FLJ92775, highly similar to *Homo sapiens* melanoma cell adhesion molecule (MCAM), mRNA(B2R642, C[+57]VASVPSIPGLN[+3]R), and aminopeptidase (Fragment)(Q59E93, AEFN[+3]ITLIHPK) in the array data of top 20 N-glycosylation sites of proteins (Fig. 8, Supplementary Table 4).

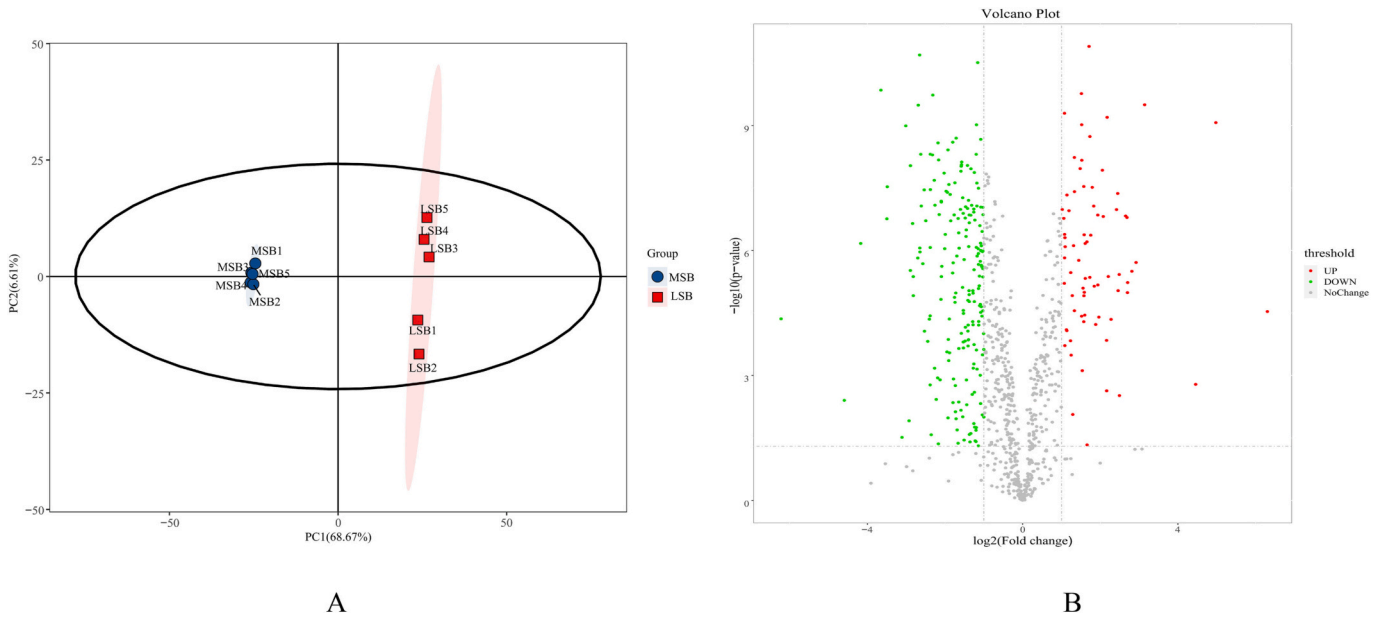

Fig. 2. N-glycosylation site analysis. A. The array data of the two group proteins were analysed using PCA. B. The volcano plot depicts the relative amounts of the modification sites in the MSB and LSB groups.

4. Discussion

The present study is the first to report N-glycosylation levels in total proteins from subchondral bone samples of patients with primary KOA. Fuehrer et al. [41] assessed N-glycosylation profiles of OA chondrocytes and fibroblast-like synovial cells. Their data suggested that the transformation of chondrocytes into the fibroblast phenotype (dedifferentiation) involved changes in N-glycosylation. Lee et al. [30] recently reported that 16 N-glycosylation profiles can be used as biomarkers for diagnosing canine OA. However, in the present study, N-glycosylation analysis of total proteins from MSB and LSB specimens from ten women with primary KOA was performed using LC-MS/MS. A total of 1149 proteins and 1369 unique N-chain glycopeptides were detected, including 1215 N-glycosylation sites, in which ptmRS scores for 1163 N-glycosylation sites were $\geq$ 0.9, as shown in Table 2. In addition, N-glycosylation in total proteins from MSB samples of patients with OA was compared with that of LSB specimens, and 295 N-glycosylation sites with significant differences were found, including 75 upregulated and 220 downregulated sites. Bioinformatics analysis of proteins with significant differences in N-glycosylation sites was subsequently performed. Analysis of sample-specific N-glycosylated proteins showed that they were mainly associated with several metabolic pathways, including extracellular matrix (ECM)-receptor interactions, focal adhesion, protein digestion and absorption, amoebiasis, and the complement and coagulation cascades. PRM validation experiments were then conducted at different sites on the selected specimens, including the MSB ($N = 5$) and LSB (N = 5). PRM experiments confirmed the N-glycosylation sites in LAMC1 (IPAIN[+3]QTITEANEK) and MXRA5(ITLHEN[+3]R), COL6A3 (VAVVQHAPSESVDN[+3]ASMPPVK), ACAN (FTFQEAAN[+3]EC[+57]R, TVYVHAN[+3]QTGYPDPSSR) B2R642 (C[+57]VASVPSIPGLN[+3]R), and Q59E93(AEFN[+3]ITLIHPK) in the array data of the top 20 N-glycosylation sites of proteins.

Changes in the total protein content in MSB and LSB samples from patients with OA may suggest the core pathogenesis of OA. Pathological alterations in the ECM in OA include a degenerated functional matrix (particularly type II collagen and proteoglycans), impaired tissue hydration, and improper synthesis of fibre ECM, accompanied by abnormal chondrocyte proliferation, senescence, inflammation, and hypertrophy [42]. Collagen fibres are the most abundant ECM constituents in connective tissues, including bones and tendons, with high control between catabolism and biosynthesis of the latter proteins to maintain homeostasis [43]. Collagen fibres generate a three-dimensional (3D) network that provides strength and toughness to the bone tissue, reducing the incidence of fractures and other diseases. Degraded subchondral collagen fibres have been detected in the weight-bearing region of the femoral head in osteonecrosis of the femoral head (ONFH) [44]. It is widely accepted that subchondral bone is involved in the development [45].

Bone remodelling allows bones to adapt to biological, mechanical, and local soluble factors, and provides an option for replacing mechanically damaged bones. With the activation of the bone remodelling process, the composition and structure of the subchondral bone undergo substantial alterations, including altered thickness of the cortical plate and changed bone mass and structure of the subchondral trabecular bone. The breakdown products of collagen fibres suppress osteoclast differentiation [46], thereby affecting remodelling of the subchondral bone. In addition, Blair-Levy et al. reported that alterations in the structure of the underlying cartilage may progressively destroy the articular cartilage, and defects in type I collagen may cause rapidly progressive OA [47]. Through PPI network analysis, it was found that collagen (COL1A1, COL2A2, COL3A1, COL4A1, COL5A2, and COL6A1) was at the core of the PPI network.

The present study revealed that the abundance of N-glycosylation of collagen was different between MSB and LSB samples, involving the COL6A3 N-glycosylation expression level of COL6A3 (VAVVQHAPSESVDN[+3]ASMPPVK), which was highly expressed in MSB samples compared to that in LSB samples from patients with primary KOA. Gu et al. [48] analysed 50 subchondral bone specimens from 40 patients with OA and 10 non-OA patients and found differential expression of COL2A1, COL5A2, COL3A1, MMP2, and COL6A1. In addition, studies have demonstrated that in patients with type II diabetes mellitus and OA, N-glycosylation of the COL6A1 protein was highly expressed [49]. Chou et al. [50] also confirmed that modification of COL5A1, COL6A3, and COL16A1 can simultaneously improve the pathological changes and disease progression of joint cartilage and subchondral bone. Abnormal glycosylation of subchondral collagen can result in trabecular bone damage and lead to subchondral bone collapse, which is highly associated with OA occurrence and development.

The present study showed that the N-glycosylation site of the ACAN protein (FTFQEAAN [+3] EC [+57] R, TVYVHAN [+3] QTGYPDPSSR)

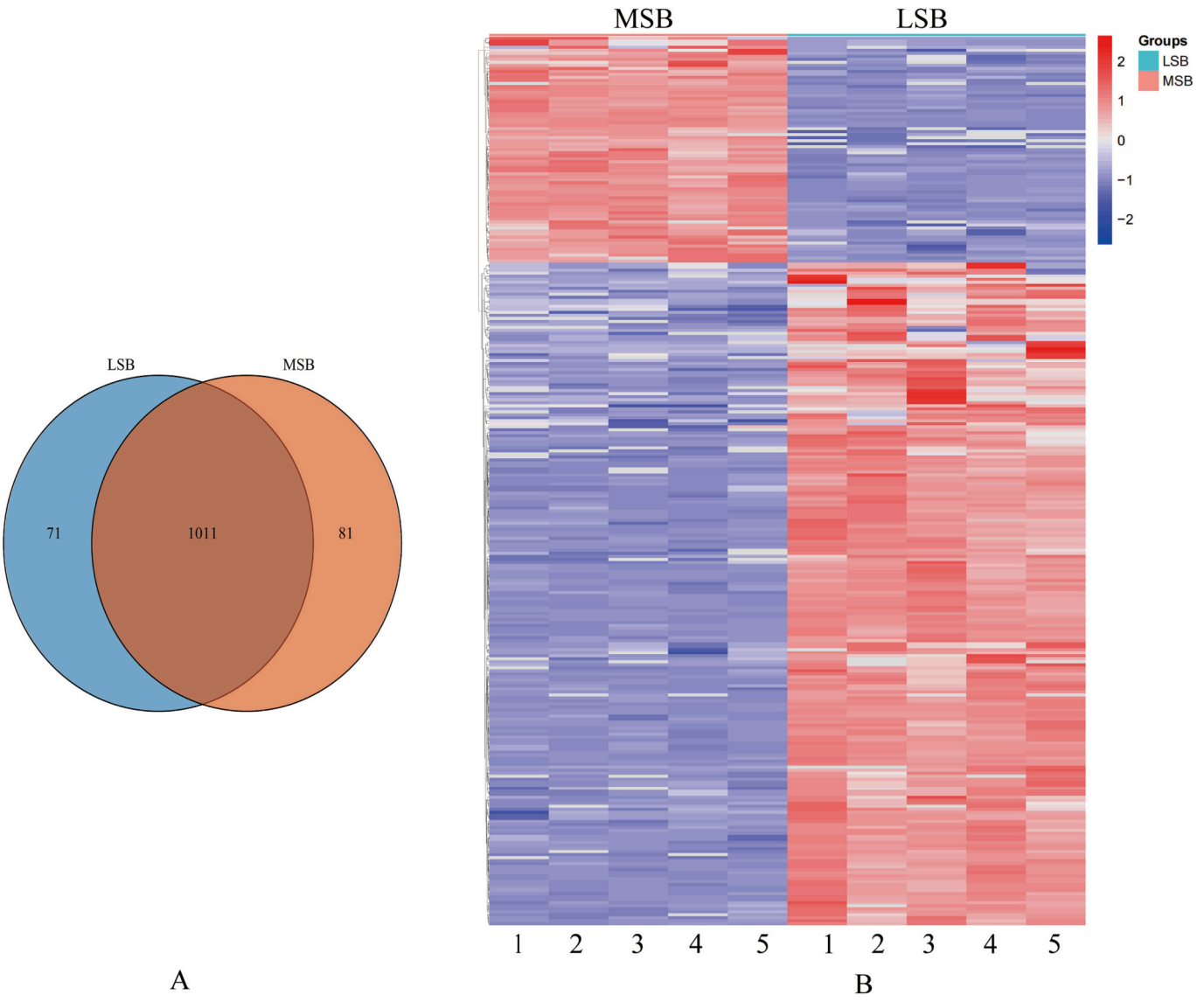

Fig. 3. Venn plot between the MSB and LSB groups. A. A comparative analysis of all ptmRS scores≥0.9. N-glycosylation sites identified between sample groups, without ensuring that signals were detected in at least three patients. B. The cluster heatmap analysis of the differences in glycosylation sites between the two groups. The screening conditions were as follows: ensuring that signals were detected in at least three patients, and then statistically analysed, in which the expression difference factor is >2 times (up and down) and the *P*-value is <0.05.

Table 2
Protein identification results.

	LSB group	MSB group	total
Protein groups	–	–	1149
Unique peptides	3342	3242	3514
N-Glycosylated peptides	1277	1283	1369
N-Glycosylation site	1127	1131	1215
N-glycosylation site ptmRS Score ≥ 0.9	1082	1092	1163

was highly expressed in the LSB compared to MSB in patients with primary KOA. PPI network analysis also found that ACAN is one of the core interacting proteins. *ACAN* gene is located on the human autosomal 15q26. 1. It can regulate the proliferation, hypertrophy, and apoptosis of chondrocytes in cartilage and bone [51,52]. Mutations of ACAN have previously been reported in patients with syndromic short stature [53,54]. Recently, Ruault et al. [55] reported that ACAN is affected by early onset OA. Zhang et al. [56] demonstrated that FBXW7 deletion in chondrocytes induced aging and accelerated cartilage catabolism, manifested by the upregulation of p16INK4A, p21, and Colx and the downregulation of Col2a1 and ACAN, resulting in the aggravation of OA. Hwang et al. [57] indicated that TGF-β1 regulated the expression

Table 3
Significant difference modification site results.

	Up regulated N-glycosylation sites **in MSB**	Down regulated N-glycosylation sites in MSB	Total number of differences N-glycosylation sites	With or without differences N-glycosylation sites
MSB vs. LSB	75	220	295	58

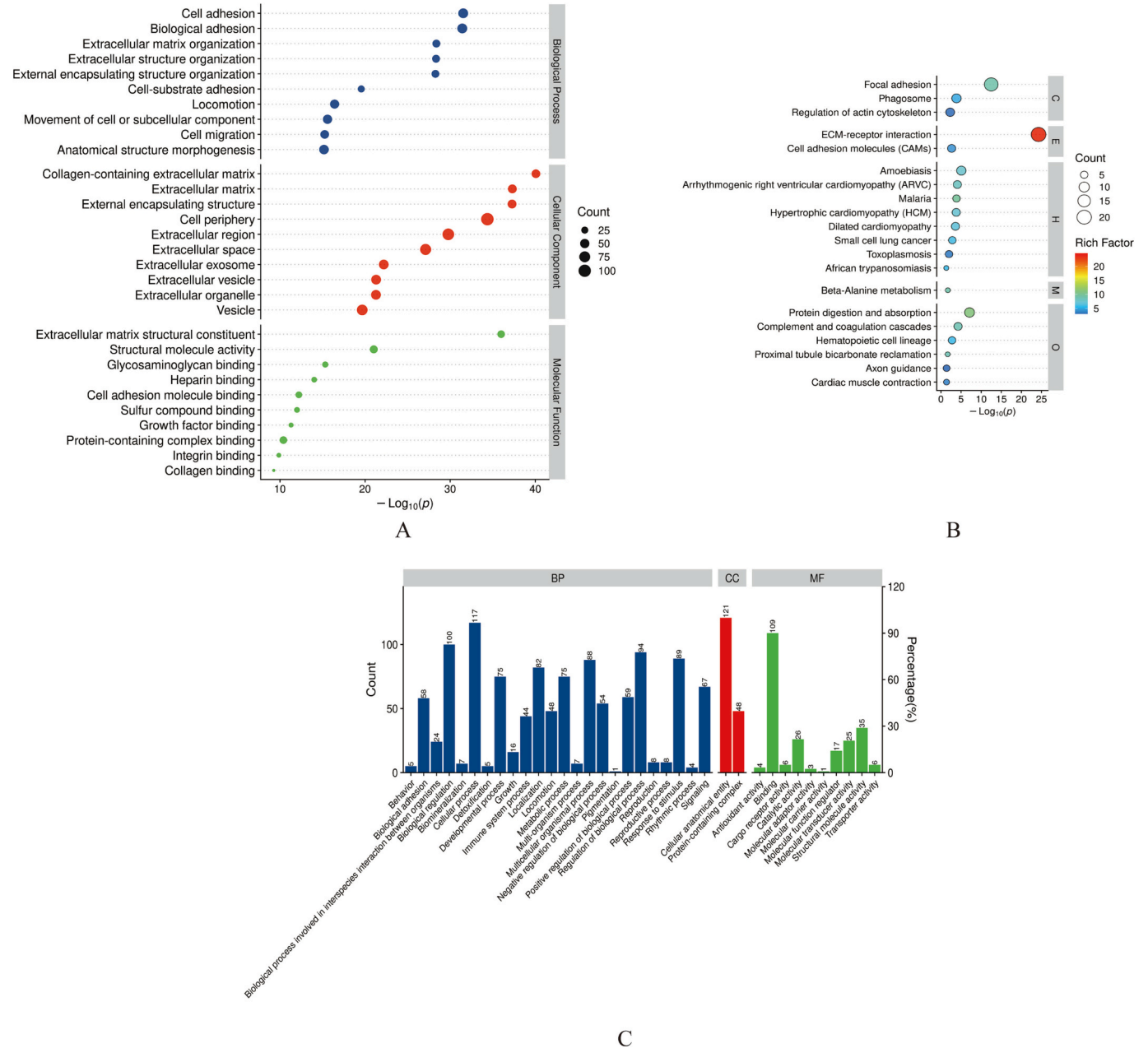

Fig. 4. Bioinformatics analysis. A. GO enrichment analysis of proteins with significantly different N-glycosylation sites. B. KEGG pathway enrichment analysis was performed to examine proteins with significantly different N-glycosylation sites. C. The annotation results of GO level 2.

levels of Col II and ACAN in chondrocytes through the Smad signalling pathway. These studies suggest that the *ACAN* gene plays an important role in the pathogenesis of OA.

The N-glycosylation site of the MXRA5 (ITLHEN[+3]R) protein was highly expressed in MSB compared to LSB of patients with primary KOA. PPI analysis revealed that it is also a core protein. Matrix reconstitution-associated protein 5 (MXRA5), an adhesion protein with leucine-rich repeats and immunoglobulin domains, has an unknown function. The MXRA family consists of three genes (MXRA5, MXRA7, and MXRA8) that may be involved in cell adhesion and matrix remodelling [58]. Balakrishnan et al. [59] employed proteomic analysis to determine the presence of MXRA5 protein in human OA synovial fluid. Lyu et al. [60] reported that the MXRA5 protein and its N-glycosylation site are associated with the pathological mechanism of Kashin-Beck disease (KBD) in identifying key proteins and N-glycosylation sites. The N-glycosylation site of the MXRA5 protein in the subchondral bone of patients with OA remains elusive and may be involved in the pathogenesis of OA.

It has also been reported that the N-glycosylation sites of LAMC1 (IPAIN[+3]QTITEANEK), B2R642 (C[+57]VASVPSIPGLN[+3]R), and Q59E93 (AEFN[+3]ITLIHPK) were different in LSB compared with those in MSB in patients with primary KOA. These three proteins and their N-glycosylation sites have not been reported in patients with OA, and their role in OA needs to be further studied. However, PPI analysis showed that the protein LAMC1 was related to the proteins ITGB1, ITGB4, ITGA3, DAG1, LAMB1, LAMB2, LAMA3, LAMA5, and NID2. It may play a role in OA and interact with these proteins.

At present, the clinical diagnosis of OA mainly relies on imaging X-rays and K-L grading, which is divided into the following grades: grade 0 (normal knee joint), grade I, grade II, grade III, and grade IV (most severe knee OA). However, diagnosis of OA using this method has entered an irreversible stage. We attempted to determine the difference in N-glycosylation site information through MSB and LSB, which may be

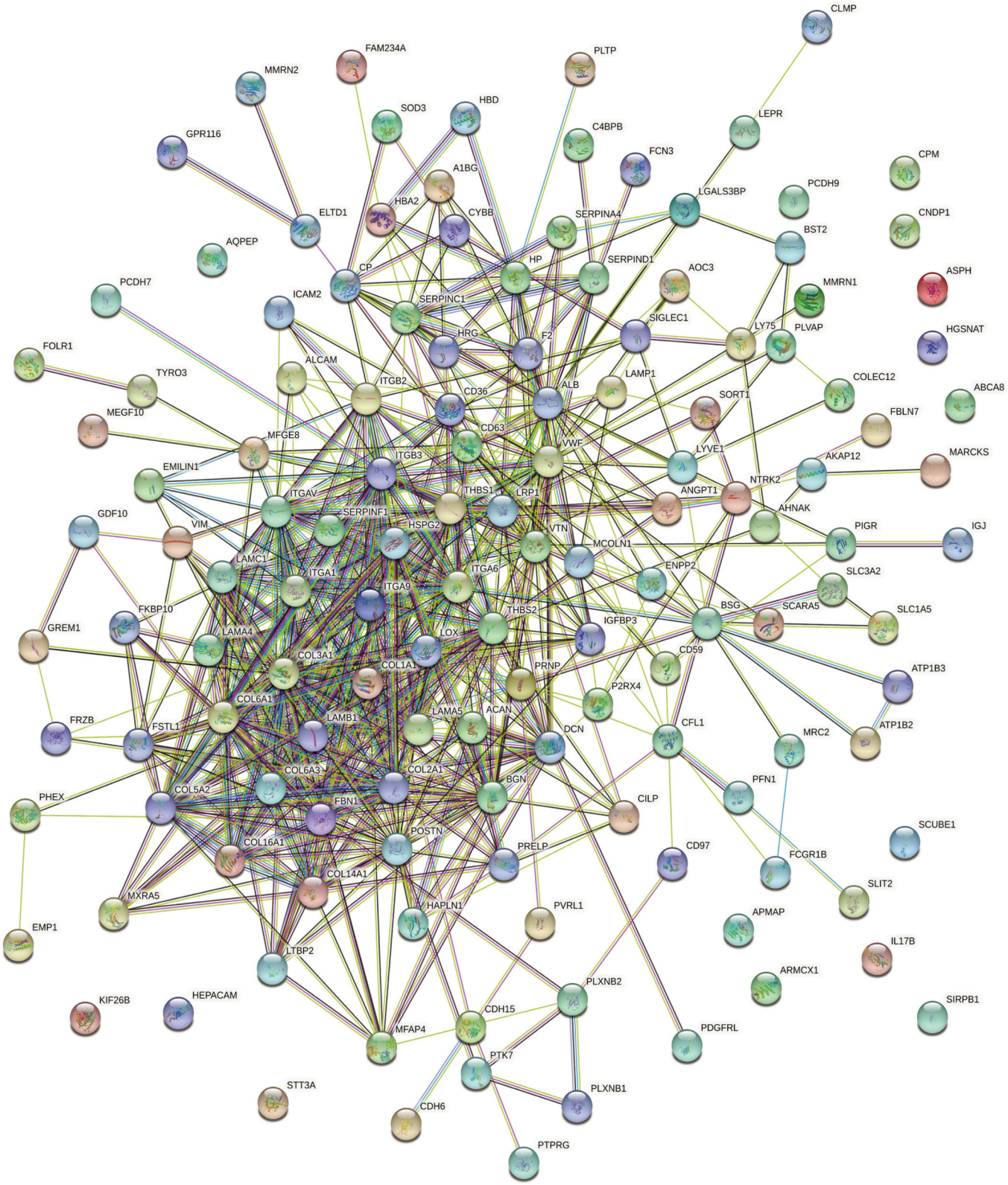

PPI

Fig. 5. Protein-protein interaction (PPI) network analysis PPI network analysis of proteins with significantly different N-glycosylation sites.

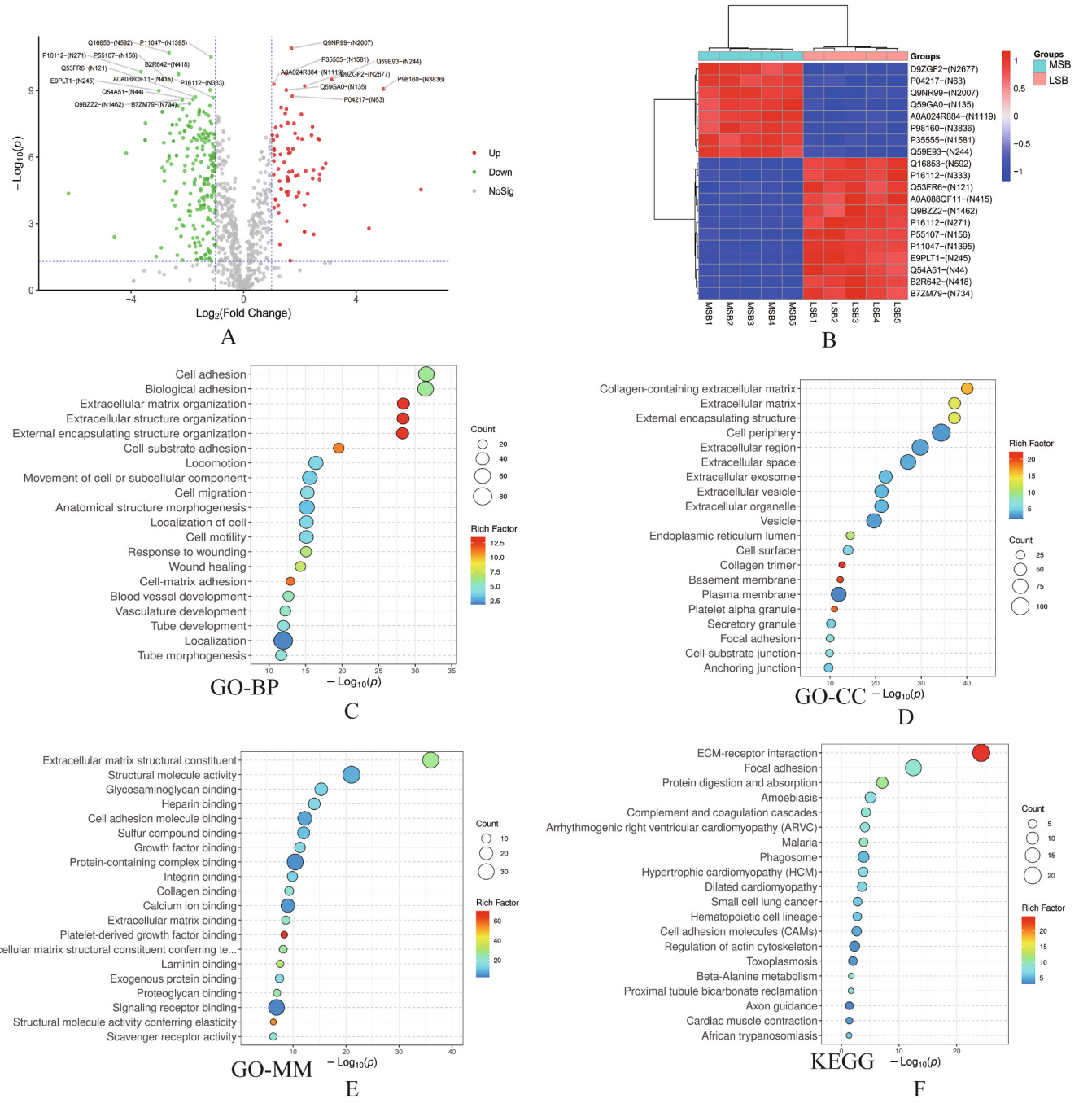

Fig. 6. Bioinformatic analysis of the top 20 N-glycosylation sites with the most significant differences A. The volcano plot of the top 20 N-glycosylation sites B. The heatmap of the top 20 N-glycosylation sites C–E. GO enrichment analyses of the top 20 N-glycosylation sites: (C) cellular component, (D) biological process, And (E) molecular function. F. KEGG enrichment analyses of the top 20 proteins.

the pathogenesis of the disease and may be the starting factor. These differential sites may enter the systemic blood through subchondral bone blood vessels and synovial fluid, and can be detected in the blood at the earliest stage of the disease to enable early detection, early treatment, and possible prevention of OA.

Although a limited number of patients were included, reflecting low statistical power, the elevated degree of consistency between the findings of the present study and those reported by other scholars confirmed the reliability of the results of this study. In addition, these findings suggest that the above-mentioned proteins could be involved in the pathogenesis of OA through N-glycosylation. Although differences in the N-glycosylation levels of MSB and LSB proteins were detected in patients with primary KOA, it remains unclear whether these differences can lead to changes in the specific functions of the proteins and how glycosylation can affect the occurrence and development of primary KOA through specific molecular mechanisms. Further studies are required to address these issues.

Study limitations: We acknowledge that our study has some limitations. First, we used studies with small sample sizes ($N = 10$) and did not conduct polycentric experiments. There are also ethical limitations, such as no appropriate control group and no sample library for N-glycosylation studies in patients with OA. Therefore, this study is not applicable to patients with OA living in different parts of the globe. Second, we selected women with primary knee OA, because these

Table 4
The array data of top 20 N-glycosylation sites of proteins.

Annotated Sequence	Protein ID	N-glycosylation site	Protein Name (Gene Symbol)	Abundance in LSB group (Mean ± SD)	Abundance in MSB group (Mean ± SD)	MSB/LSB (p value)	MSB/LSB (Fold change)
[R].ITLHENR.[T]	Q9NR99	N2007	Matrix-remodelling-associated protein 5 (MXRA5)	1,777,613.1 ± 123,149.3	5,812,880.3 ± 106,766.3	<0.001	3.27
[R].YLYLASNHSNK.[W]	Q16853	N592	Membrane primary amine oxidase (AOC3)	350,592,629.6 ± 11,701,288.1	55,682,836.5 ± 4,781,471.5	<0.001	0.16
[K].IPAINQTITEANEK.[T]	P11047	N1395	Laminin subunit gamma-1 (LAMC1)	72,353,705.5 ± 1,566,970.7	32,406,894.5 ± 896,026.6	<0.001	0.45
[K].FTFQEAANECR.[R]	P16112	N271	Aggrecan core protein (ACAN)	19,883,088.7 ± 986,232.7	1,580,692.3 ± 171,271.2	<0.001	0.08
[K].AWGTPCEMCPAVNTSEYK.[I]	P35555	N1581	Fibrillin-1 (FBN1)	1,865,488.4 ± 105,661.4	5,327,037.2 ± 162,573.3	<0.001	2.86
[R].CVASVPSIPGLNR.[T]	B2R642	N418	cDNA, FLJ92775, highly similar to *Homo sapiens* melanoma cell adhesion molecule (MCAM), mRNA	12,232,498.6 ± 542,088.0	2,457,253.9 ± 110,246.9	<0.001	0.2
[K].AEFNITLIHPK.[D]	Q59E93	N244	Aminopeptidase (Fragment)	2,013,915.2 ± 495,784.4	17,783,744.1 ± 815,738.7	<0.001	8.83
[K].NASGRPLPLGPPTR.[Q]	P55107	N156	Growth/differentiation factor 10(GDF10)	1,409,122.3 ± 63,562.0	218,329.8 ± 34,408.6	<0.001	0.15
[RH].NLTVPGSLR.[AS]	A0A024R884	N1119	Tenascin C (Hexabrachion), isoform CRA_a (TNC)	27,852,395.9 ± 950,906.1	58,757,112.8 ± 1,741,994.9	<0.001	2.11
[R].VAVVQHAPSESVDNASMPPVK.[V]	D9ZGF2	N2677	Collagen, type VI, alpha 3 (COL6A3)	2,549,377.3 ± 268,433.4	11,520,262.2 ± 528,327.2	<0.001	4.52
[R].IQGEEIVFHDLNLTAHGISHCPTCR.[D]	P98160	N3836	Basement membrane-specific heparan sulphate proteoglycan core protein (HSPG2)	1,095,075.9 ± 964,304.5	34,478,451.9 ± 2,074,820.3	<0.001	3.15
[K].DEGTYTCALHHSGHSPPISSQNVTVLR.[GD]	Q59GA0	N135	Thy-1 antigen (Fragment)	6,813,270.3 ± 375,533.9	19,539,665.2 ± 801,407.2	<0.001	2.87
[R].TVYVHANQTGYPDPSSR.[Y]	P16112	N333	Aggrecan core protein (ACAN)	1,112,482,733 ± 36,804,079.1	487,720,477.4 ± 23,118,213.1	<0.001	0.44
[K].IISKNCTSYGVLDISK.[C]	E9PLT1	N245	Glycoprotein IIIb (CD36)	46,701,491.6 ± 2,839,708.9	5,790,304.2 ± 396,728.4	<0.001	0.12
[K].NGVAQEPVHLDSPAIK.[H]	P04217	PN63	Alpha-1B-glycoprotein (A1BG)	3,276,180.5 ± 434,839.8	10,882,219.3 ± 374,958.3	<0.001	3.32
[R].CGPCPAGFTGNGSHCTDVNECNAHPCFPR.[V]	Q53FR6	N121	Cartilage oligomeric matrix protein variant (Fragment)	42,712,334.9 ± 1,894,451.8	14,832,075.7 ± 1,245,373.1	<0.001	0.3
[K].TCNPETFPSSNESR.[Q]	A0A088QF11	N415	Choline transporter-like protein 2 isoform 2 (SLC44A2)	35,169,569.4 ± 1,382,131.1	16,641,852.6 ± 354,031.9	<0.001	0.47
[K].ILLTCSLNDSATEVTGHR.[W]	Q54A51	N44	Basigin)hEMMPRIN)	64,095,030.5 ± 3,510,655.2	18,378,783.5 ± 750,884.4	<0.001	0.29
[R].VVAEPGLDVPEGAALNLSCR.[L]	Q9BZZ2	N1462	Sialoadhesin(SIGLEC1)	3,754,933.5 ± 227,983.0	827,904.6 ± 37,262.7	<0.001	0.22
[R].IDPVTGNITLEEKPAPTDVGLHR.[L]	B7ZM79	N734	PCDH9 protein(PCDH9)	2,739,540.9 ± 162,920.8	721,385.8 ± 37,783.8	<0.001	0.26

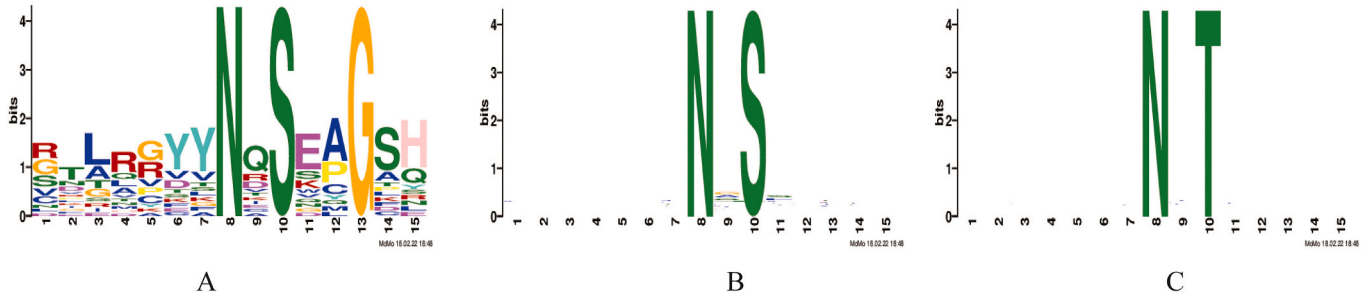

Fig. 7. Motif analysis of differences N-glycosylation sites. Sequence analysis was performed on the identified N-glycosylation sites from positions 1–15. A: *p*-value = 1.4e-32, B: p-value = 3.1e-5, and C: p-value = 5.0e-18. N-glycosylated peptide motif analysis showed that the difference in N-glycosylation sites was mainly concentrated in position 8.

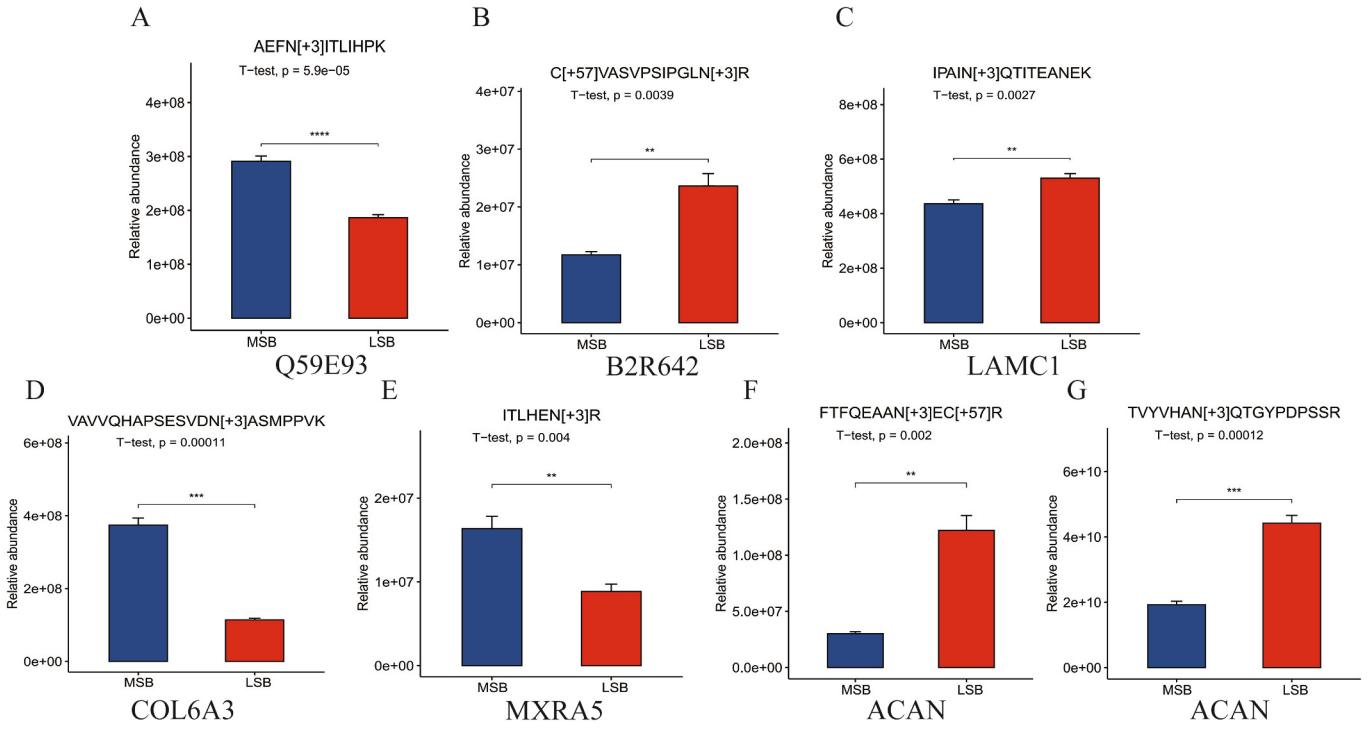

Fig. 8. PRM experiments confirmed the N-glycosylation sites of the proteins.

individuals were more likely to have knee OA. Men with OA may have different metabolic levels from women, resulting in a bias in the findings of this study. Finally, we only analysed primary KOA and did not compare people with other secondary OA, such as rheumatic OA or traumatic OA. The underlying mechanisms of disease aetiology and pathology differ in both settings, and our study cannot be applied to all types of OA.

5. Conclusions

N-Glycosylation may be associated with the development of OA. However, it is essential to clarify the glycosylation mechanism and the role of N-glycosylation in OA. In the present study, we detected the total protein N-glycosylation levels of MSB and LSB samples from patients with primary KOA and found 295 N-glycosylation sites with significant differences. PRM validation experiments were conducted on seven different sites of selected specimens; although these sites with significant differences require further validation, proteins with differences in N-glycosylation sites may be influential factors causing the imbalance of bone metabolism in the subchondral bone. The specific mechanisms underlying the development of these diseases require further exploration. It is also an interesting study to compare the changes in N-glycosylation during OA progression in the future.

Supplementary data to this article can be found online at https://doi.org/10.1016/j.jprot.2023.104896.

Significance

Our study showed that protein N-glycosylation modifications are involved in the development of primary KOA, and the identified differential N-glycosylation sites may be one of the causes of KOA subchondral bone metabolism imbalance. It provides new data for future studies of N-glycosylation modification proteomics of KOA and provides potential biological markers for the diagnosis and treatment of primary KOA.

Author contributions

Qunhua Jin and Zhidong Lu designed the experiment. Gangning Feng and Yong Zhou carried out the studies, participated in collecting

data, and drafted the manuscript. Gangning Feng, Yong Yang and Jiangbo Yan performed the statistical analysis and participated in its design. Gangning Feng Weidong Zhao, Na Wang and Zheng Wang participated in acquisition, analysis, or interpretation of data and draft the manuscript. All authors read and approved the final manuscript.

Funding

The National Natural Science Foundation of China (N0.U22A20285) and the National Natural Science Foundation of China (No. 82060331). The work was supported by the Scientifific Research Project from Ningxia Province (No.2021A0478), the Natural Science Foundation of Ningxia (No. 2020AAC03123).the Scientifific Research Project from Ningxia Medical University, (No.XT2021010).

Declaration of Competing Interest

All authors declare that they have no conflicts of interest to this work.

Data availability

Data will be made available on request.

Acknowledgments

We would like to thank MedSci for English language editing. We also thank Gaolong Yin at Shanghai Bioprofile Technology Company Ltd. for his technical support in proteomics.

References

[1] J.G. Quicke, P.G. Conaghan, N. Corp, G. Peat, Osteoarthritis year in review 2021: epidemiology & therapy, Osteoarthr. Cartil. 30 (2022) 196–206.
[2] D. Li, S. Li, Q. Chen, X. Xie, The prevalence of symptomatic knee osteoarthritis in relation to age, sex, area, region, and body mass index in China: a systematic review and meta-analysis, Front. Med. (Lausanne) 7 (2020) 304.
[3] X. Tang, S. Wang, S. Zhan, J. Niu, K. Tao, Y. Zhang, et al., The prevalence of symptomatic knee osteoarthritis in China: results from the China health and retirement longitudinal study, Arthritis Rheum. 68 (2016) 648–653.
[4] S. Suri, D.A. Walsh, Osteochondral alterations in osteoarthritis, Bone 51 (2012) 204–211.
[5] W. Hu, Y. Chen, C. Dou, S. Dong, Microenvironment in subchondral bone: predominant regulator for the treatment of osteoarthritis, Ann. Rheum. Dis. 80 (2021) 413–422.
[6] T. Hügle, J. Geurts, What drives osteoarthritis?-synovial versus subchondral bone pathology, Rheumatology (Oxford) 56 (2017) 1461–1471.
[7] D.B. Burr, A. Utreja, Editorial: Wnt signaling related to subchondral bone density and cartilage degradation in osteoarthritis, Arthritis Rheum. 70 (2018) 157–161.
[8] K. Liu, Y. Chen, Y. Miao, F. Xue, J. Yin, L. Wang, et al., Microstructural and histomorphological features of osteophytes in late-stage human knee osteoarthritis with varus deformity, Joint Bone Spine 89 (2022) 105353.
[9] A. Varki, Biological roles of oligosaccharides: all of the theories are correct, Glycobiology 3 (1993) 97–130.
[10] H. Lis, N. Sharon, Protein glycosylation. Structural and functional aspects, Eur. J. Biochem. 218 (1993) 1–27.
[11] M.R. Wormald, R.A. Dwek, Glycoproteins: glycan presentation and protein-fold stability, Structure 7 (1999) R155–R160.
[12] A. Kobata, Structures and functions of the sugar chains of glycoproteins, Eur. J. Biochem. 209 (1992) 483–501.
[13] J.N. Arnold, R. Saldova, U.M. Hamid, P.M. Rudd, Evaluation of the serum N-linked glycome for the diagnosis of cancer and chronic inflammation, Proteomics 8 (2008) 3284–3293.
[14] N.H. Packer, C.W. von der Lieth, K.F. Aoki-Kinoshita, C.B. Lebrilla, J.C. Paulson, R. Raman, et al., Frontiers in glycomics: bioinformatics and biomarkers in disease. An NIH white paper prepared from discussions by the focus groups at a workshop on the NIH campus, Bethesda MD (September 11-13, 2006), Proteomics 8 (2008) 8–20.
[15] C.B. Lebrilla, H.J. An, The prospects of glycan biomarkers for the diagnosis of diseases, Mol. BioSyst. 5 (2009) 17–20.
[16] L.R. Ruhaak, S. Miyamoto, C.B. Lebrilla, Developments in the identification of glycan biomarkers for the detection of cancer, Mol. Cell. Proteomics 12 (2013) 846–855.
[17] B. Adamczyk, T. Tharmalingam, P.M. Rudd, Glycans as cancer biomarkers, Biochim. Biophys. Acta (2012) 1347–1353.
[18] S.S. Pinho, C.A. Reis, Glycosylation in cancer: mechanisms and clinical implications, Nat. Rev. Cancer 15 (2015) 540–555.
[19] J.R. Wang, W.N. Gao, R. Grimm, S. Jiang, Y. Liang, H. Ye, et al., A method to identify trace sulfated IgG N-glycans as biomarkers for rheumatoid arthritis, Nat. Commun. 8 (2017) 631.
[20] F. Clerc, M. Novokmet, V. Dotz, K.R. Reiding, N. de Haan, G.S.M. Kammeijer, et al., Plasma N-glycan signatures are associated with features of inflammatory bowel diseases, Gastroenterology 155 (2018) 829–843.
[21] J. Martel-Pelletier, A.J. Barr, F.M. Cicuttini, P.G. Conaghan, C. Cooper, M. B. Goldring, et al., Osteoarthritis, Nat. Rev. Dis. Primers 2 (2016) 16072.
[22] O.H. Jeon, D.R. Wilson, C.C. Clement, S. Rathod, C. Cherry, B. Powell, et al., Senescence cell-associated extracellular vesicles serve as osteoarthritis disease and therapeutic markers, JCI Insight 4 (2019).
[23] K. Fu, S.R. Robbins, J.J. McDougall, Osteoarthritis: the genesis of pain, Rheumatology (Oxford) 57 (2018) iv43–iv50.
[24] R.F. Loeser, J.A. Collins, B.O. Diekman, Ageing and the pathogenesis of osteoarthritis, Nat. Rev. Rheumatol. 12 (2016) 412–420.
[25] E. Klaver, P. Zhao, M. May, H. Flanagan-Steet, H.H. Freeze, R. Gilmore, et al., Selective inhibition of N-linked glycosylation impairs receptor tyrosine kinase processing, Dis. Model. Mech. 12 (2019).
[26] H. Yasuda, N. Shima, N. Nakagawa, S.I. Mochizuki, K. Yano, N. Fujise, et al., Identity of osteoclastogenesis inhibitory factor (OCIF) and osteoprotegerin (OPG): a mechanism by which OPG/OCIF inhibits osteoclastogenesis in vitro, Endocrinology 139 (1998) 1329–1337.
[27] W.S. Simonet, D.L. Lacey, C.R. Dunstan, M. Kelley, M.S. Chang, R. Lüthy, et al., Osteoprotegerin: a novel secreted protein involved in the regulation of bone density, Cell 89 (1997) 309–319.
[28] E. Tsuda, M. Goto, S. Mochizuki, K. Yano, F. Kobayashi, T. Morinaga, et al., Isolation of a novel cytokine from human fibroblasts that specifically inhibits osteoclastogenesis, Biochem. Biophys. Res. Commun. 234 (1997) 137–142.
[29] T. Matsuhashi, N. Iwasaki, H. Nakagawa, M. Hato, M. Kurogochi, T. Majima, et al., Alteration of N-glycans related to articular cartilage deterioration after anterior cruciate ligament transection in rabbits, Osteoarthr. Cartil. 16 (2008) 772–778.
[30] H. Lee, A. Lee, N. Seo, J. Oh, O.K. Kweon, H.J. An, et al., Discovery of N-glycan biomarkers for the canine osteoarthritis, Life (Basel) 10 (2020).
[31] S. Ahlbäck, Osteoarthrosis of the knee. A radiographic investigation, Acta Radiol. Diagn. (Stockh) Suppl 277 (1968) 7–72.
[32] J.S. Hernborg, B.E. Nilsson, The natural course of untreated osteoarthritis of the knee, Clin. Orthop. Relat. Res. (1977) 130–137.
[33] D.F. Zielinska, F. Gnad, K. Schropp, J.R. Wiśniewski, M. Mann, Mapping N-glycosylation sites across seven evolutionarily distant species reveals a divergent substrate proteome despite a common core machinery, Mol. Cell 46 (2012) 542–548.
[34] I. Chamrád, O. Strouhal, P. Rehulka, R. Lenobel, M. Sebela, Microscale affinity purification of trypsin reduces background peptides in matrix-assisted laser desorption/ionization mass spectrometry of protein digests, J. Proteome 74 (2011) 948–957.
[35] J.M. Burkhart, C. Schumbrutzki, S. Wortelkamp, A. Sickmann, R.P. Zahedi, Systematic and quantitative comparison of digest efficiency and specificity reveals the impact of trypsin quality on MS-based proteomics, J. Proteome 75 (2012) 1454–1462.
[36] J. Rappsilber, M. Mann, Y. Ishihama, Protocol for micro-purification, enrichment, pre-fractionation and storage of peptides for proteomics using StageTips, Nat. Protoc. 2 (2007) 1896–1906.
[37] A.C. Peterson, J.D. Russell, D.J. Bailey, M.S. Westphall, J.J. Coon, Parallel reaction monitoring for high resolution and high mass accuracy quantitative, targeted proteomics, Mol. Cell. Proteomics 11 (2012) 1475–1488.
[38] B. MacLean, D.M. Tomazela, N. Shulman, M. Chambers, G.L. Finney, B. Frewen, et al., Skyline: an open source document editor for creating and analyzing targeted proteomics experiments, Bioinformatics 26 (2010) 966–968.
[39] J.K. Eng, B.C. Searle, K.R. Clauser, D.L. Tabb, A face in the crowd: recognizing peptides through database search, Mol. Cell. Proteomics 10 (2011). R111.009522.
[40] S. Tyanova, T. Temu, J. Cox, The MaxQuant computational platform for mass spectrometry-based shotgun proteomics, Nat. Protoc. 11 (2016) 2301–2319.
[41] J. Fuehrer, K.M. Pichler, A. Fischer, A. Giurea, D. Weinmann, F. Altmann, et al., N-glycan profiling of chondrocytes and fibroblast-like synoviocytes: towards functional glycomics in osteoarthritis, Proteomics Clin. Appl. 15 (2021), e2000057.
[42] T. Pap, A. Korb-Pap, Cartilage damage in osteoarthritis and rheumatoid arthritis - two unequal siblings, Nat. Rev. Rheumatol. 11 (2015) 606–615.
[43] J. Halper, M. Kjaer, Basic components of connective tissues and extracellular matrix: elastin, fibrillin, fibulins, fibrinogen, fibronectin, laminin, tenascins and thrombospondins, Adv. Exp. Med. Biol. 802 (2014) 31–47.
[44] Z. Wu, B. Wang, J. Tang, B. Bai, S. Weng, Z. Xie, et al., Degradation of subchondral bone collagen in the weight-bearing area of femoral head is associated with osteoarthritis and osteonecrosis, J. Orthop. Surg. Res. 15 (2020) 526.
[45] D.M. Findlay, J.S. Kuliwaba, Bone-cartilage crosstalk: a conversation for understanding osteoarthritis, Bone Res. 4 (2016) 16028.
[46] D. Pfander, T. Cramer, D. Deuerling, G. Weseloh, B. Swoboda, Expression of thrombospondin-1 and its receptor CD36 in human osteoarthritic cartilage, Ann. Rheum. Dis. 59 (2000) 448–454.
[47] J.M. Blair-Levy, C.E. Watts, N.M. Fiorentino, E.K. Dimitriadis, J.C. Marini, P. E. Lipsky, A type I collagen defect leads to rapidly progressive osteoarthritis in a mouse model, Arthritis Rheum. 58 (2008) 1096–1106.
[48] H.Y. Gu, M. Yang, J. Guo, C. Zhang, L.L. Lin, Y. Liu, et al., Identification of the biomarkers and pathological process of osteoarthritis: weighted gene co-expression network analysis, Front. Physiol. 10 (2019) 275.

[49] Y. Luo, Z. Wu, S. Chen, H. Luo, X. Mo, Y. Wang, et al., Protein N-glycosylation aberrations and glycoproteomic network alterations in osteoarthritis and osteoarthritis with type 2 diabetes, Sci. Rep. 12 (2022) 6977.
[50] C.H. Chou, C.H. Lee, L.S. Lu, I.W. Song, H.P. Chuang, S.Y. Kuo, et al., Direct assessment of articular cartilage and underlying subchondral bone reveals a progressive gene expression change in human osteoarthritic knees, Osteoarthr. Cartil. 21 (2013) 450–461.
[51] P.J. Roughley, J.S. Mort, The role of aggrecan in normal and osteoarthritic cartilage, J. Exp. Orthop. 1 (2014) 8.
[52] Y.W. Koh, S.M. Chun, Y.S. Park, J.S. Song, G.K. Lee, S.K. Khang, et al., Association between the CpG island methylator phenotype and its prognostic significance in primary pulmonary adenocarcinoma, Tumour Biol. 37 (2016) 10675–10684.
[53] L. Gleghorn, R. Ramesar, P. Beighton, G. Wallis, A mutation in the variable repeat region of the aggrecan gene (AGC1) causes a form of spondyloepiphyseal dysplasia associated with severe, premature osteoarthritis, Am. J. Hum. Genet. 77 (2005) 484–490.
[54] E.L. Stattin, F. Wiklund, K. Lindblom, P. Onnerfjord, B.A. Jonsson, Y. Tegner, et al., A missense mutation in the aggrecan C-type lectin domain disrupts extracellular matrix interactions and causes dominant familial osteochondritis dissecans, Am. J. Hum. Genet. 86 (2010) 126–137.
[55] V. Ruault, K. Yauy, A. Fabre, M. Fradin, J. Van-Gils, C. Angelini, et al., Clinical and molecular Spectrum of nonsyndromic early-onset osteoarthritis, Arthritis Rheum. 72 (2020) 1689–1693.
[56] H. Zhang, Y. Shao, Z. Yao, L. Liu, H. Zhang, J. Yin, et al., Mechanical overloading promotes chondrocyte senescence and osteoarthritis development through downregulating FBXW7, Ann. Rheum. Dis. 81 (2022) 676–686.
[57] H.S. Hwang, M.H. Lee, H.A. Kim, TGF-β1-induced expression of collagen type II and ACAN is regulated by 4E-BP1, a repressor of translation, FASEB J. 34 (2020) 9531–9546.
[58] A. Gabrielsen, P.R. Lawler, W. Yongzhong, D. Steinbrüchel, D. Blagoja, G. Paulsson-Berne, et al., Gene expression signals involved in ischemic injury, extracellular matrix composition and fibrosis defined by global mRNA profiling of the human left ventricular myocardium, J. Mol. Cell. Cardiol. 42 (2007) 870–883.
[59] L. Balakrishnan, R.S. Nirujogi, S. Ahmad, M. Bhattacharjee, S.S. Manda, S. Renuse, et al., Proteomic analysis of human osteoarthritis synovial fluid, Clin. Proteomics 11 (2014) 6.
[60] Y. Lyu, H. Deng, C. Qu, L. Qiao, X. Liu, X. Xiao, et al., Identification of proteins and N-glycosylation sites of knee cartilage in Kashin-Beck disease compared with osteoarthritis, Int. J. Biol. Macromol. 210 (2022) 128–138.